JOURNAL OF BACTERIOLOGY, Aug. 2011, p. 4180–4191 Vol. 193, No. 16
0021-9193/11/$12.00 doi:10.1128/JB.00385-11

Genetic and Biochemical Analysis of PadR-*padC* Promoter Interactions during the Phenolic Acid Stress Response in *Bacillus subtilis* 168▽¶

Thi Kim Chi Nguyen,†‡ Ngoc Phuong Tran,†§ and Jean-François Cavin*

Laboratoire GPMA, IFR92, AgroSup Dijon, Université de Bourgogne, 1 Esplanade Erasme, F-21000 Dijon, France

Received 22 March 2011/Accepted 6 June 2011

***Bacillus subtilis* 168 is resistant to phenolic acids by expression of an inducible enzyme, the phenolic acid decarboxylase (PadC), that decarboxylates these acids into less toxic vinyl derivatives. In the phenolic acid stress response (PASR), the repressor of *padC*, PadR, is inactivated by these acids. Inactivation of PadR is followed by a strong expression of *padC*. To elucidate the functional interaction between PadR and the *padC* promoter, we performed (i) footprinting assays to identify the region protected by PadR, (ii) electrophoretic mobility shift assays (EMSAs) with a modified *padC* promoter protected region to determine the interacting sequences, and (iii) random mutagenesis of *padR* to identify amino acid residues essential for the function of PadR. We identified an important consensus dyad sequence called IR1-2 (ATGT-8N-ACAT) overlapping a second dyad element (GTGT-8N-ACAT) that we named dIR1-2bis. The entire dIR1-2bis/IR1-2 sequence permits binding of two PadR dimers in EMSAs, which may be observed for bacteria grown under noninduced conditions where the *padC* promoter is completely repressed. Three groups of modified PadRs giving a PASR phenotype were characterized *in vivo*. The DNA sequences of certain mutant *padR* alleles indicate that important residues are all located in the region containing the coiled-coil leucine zipper domain that is involved in dimerization. These substitutions reduce the affinity of PadR binding to the *padC* promoter. Of particular interest are residue L128, located at the center of the putative coiled-coil leucine zipper domain, and residue E97, which is conserved among all PadRs.**

Phenolic acids (also termed substituted hydroxycinnamic acids) are naturally abundant plant compounds with important roles as lignin-related aromatic acids. These acids can be released by cinnamonyl esterase activities, which are expressed by various microorganisms (10, 12, 27) and in their free form induce a specific chemical stress response in microorganisms. Certain bacteria, such as the probiotic organism *Lactobacillus plantarum* (6, 8, 15), *Pediococcus pentosaceus* (7), and *Bacillus subtilis* (9, 29, 32), are resistant to the toxicity of phenolic acids, such as ferulic, *p*-coumaric, and caffeic acids. This resistance is due to the rapid induction of the *padA* or *padC* gene, which encodes a phenolic acid decarboxylase (PadA or PadC) that can rapidly degrade these antimicrobial acids into less toxic vinyl derivatives (6). This resistance mechanism is termed the phenolic acid stress response (PASR) (32). In *B. subtilis* 168, the expression of *padC*, which is cotranscribed with upstream noncharacterized and supposedly nonfunctional *yveFG* genes (29, 32) (Fig. 1), is controlled by a negative transcriptional regulator (PadR) that was identified as the first member of what is now a large family of transcriptional regulators (Pflam PF03551) (7, 14). This family, which is subdivided into two distinct subfamilies (17), consists of more than 2,800 entries in GenBank for completed genomes or running sequencing projects. PF03551 belongs to the gluconate operon repressor (GntR) superfamily, whose members possess an alpha C-terminal core. To date, the function is known for only a few members of the PadR family, which have been shown to play a major role in the biology of their host bacteria. Among these members, (i) AphA from *Vibrio cholerae* is a quorum sensing-regulated activator that initiates the virulence cascade and is a repressor of penicillin amidase activity (*pva* gene) (18, 19, 20, 23), (ii) LadR from *Listeria monocytogenes* negatively regulates the expression of the multidrug efflux pump MdrL (17), (iii) LstR is required for effective thermal resistance (35), and (iv) LmrR from *Lactococcus lactis* regulates the production of LmrCD, a major multidrug ABC transporter (1, 25). Crystal structures of two PadR-like proteins, AphA (11) and Pex (5), revealed a protein structure containing a conserved N-terminal winged helix-turn-helix (WHTH) that acts as the DNA-binding motif (4). This protein architecture is similar to that of the repressor MarR, which controls antibiotic resistance (2), and further shows the existence of a highly divergent C-terminal domain involved in dimerization. Since to our knowledge the existence of a putative PASR has not been investigated in these species, the biochemical characteristics of initially described PadRs have not been studied. In the PASR, PadR binds to the *padC* promoter to repress the expression of *padC* in the absence of phenolic acids (32), but the site of interaction

* Corresponding author. Mailing address: Laboratoire GPMA, IFR92, AgroSup Dijon, Université de Bourgogne, 1 Esplanade Erasme, F-21000 Dijon, France. Phone: (33) 3 80 77 40 72. Fax: (33) 3 80 77 23 84. E-mail: cavinjf@u-bourgogne.fr.

¶ Supplemental material for this article may be found at http://jb.asm.org/.

† T. K. C. Nguyen and N. P. Tran contributed equally to this work.

‡ Present address: UMR Université-INRA 0483, Laboratoire de l'Immunologie Parasitaire, Vaccinologie et Biothérapie Anti-Infectieuse, UFR de Pharmacie, 31 Avenue Monge, 37200 Tours, France.

§ Present address: UMR CNRS 2472-INRA 1157, Virologie Moléculaire et Structurale, 1 Avenue de la Terrasse, 91198 Gif-sur-Yvette, France.

▽ Published ahead of print on 17 June 2011.

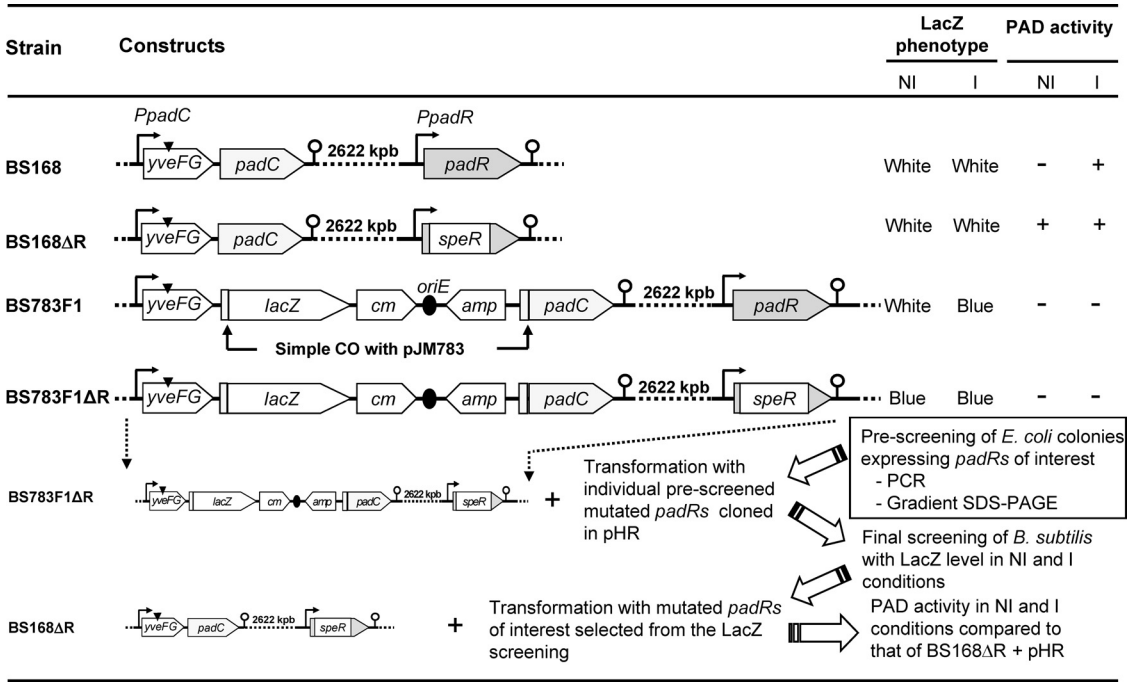

FIG. 1. Construction and phenotypes of *B. subtilis* 168 mutant strains. This includes the strategy used to screen for mutant *padR* genes obtained by complementation of a *padR* mutant strain (BS783F1ΔR). The black triangle shown above *yveFG* indicates the stop codon (32). NI, noninduced; I, induced by 1 mM ferulic acid. An absence of PAD activity in the induced fusion strain 783F1 results from the absence of the promoter region upstream of the *padC* gene.

and amino acid residues involved in the functionality of PadR are unknown.

In this work, we identify for the first time the necessary sequences of the *padC* promoter involved in the interaction with PadR. We also identify single amino acid substitutions that modify the function of PadR. Results from electrophoretic mobility shift assays (EMSAs) with native and modified *padC* promoters and modified PadR were supported by *in vivo* experiments using wild-type *B. subtilis* 168 and a *padR* mutant strain.

MATERIALS AND METHODS

Bacterial strains and growth conditions. Bacterial strains and plasmids used in this study are listed in Table 1. *Escherichia coli*, *B. subtilis* 168, and corresponding mutant strains were grown aerobically in Erlenmeyer flasks on a rotary shaker in Luria-Bertani (LB) medium at 37°C. For selection and growth, antibiotics were used at the following concentrations: erythromycin, 100 μg/ml for *E. coli* and 5 μg/ml for *B. subtilis* 168; chloramphenicol, 5 μg/ml for *B. subtilis* 168; ampicillin, 200 μg/ml; and kanamycin, 50 μg/ml for *E. coli.*

DNA extraction, PCR amplification, sequencing, bacterial transformation, and bioinformatic analysis. Standard molecular procedures were used as described by Sambrook et al. (31). Genomic DNA was extracted as described previously (32). PCR amplifications were performed in 50-μl reaction mixtures, using 0.1 unit of Platinum high-fidelity *Taq* DNA polymerase (Invitrogen) in a thermocycler (Bio-Rad) with the primers (Eurogentec) listed in Table 2. PCR products and digested DNA fragments were purified using either a QIAquick PCR purification kit or a QIAgel agarose gel extraction kit (Qiagen). *E. coli* was transformed by electroporation as described by Dower et al. (13). *B. subtilis* 168 was transformed with linear plasmid DNA or chromosomal DNA by using a two-step nutrient downshift as previously described (28). DNA sequences (Cogenic) were analyzed using Bio-Edit software.

DNase I footprinting assays. DNase I protection assays were performed as previously described (22). Briefly, a 234-bp probe (P1), encompassing positions −97 to +137 relative to the transcription start site of the *padC* promoter (see Fig. 3), was produced by PCR amplification with primer BSD1 or BSD8 (Table 2) previously labeled with T4 polynucleotide kinase (Invitrogen) in the presence of [γ-^{32}P]ATP (Perkin-Elmer). The probe-PadR protein binding reactions were conducted under the conditions for EMSA (see below), with 0.1 to 10 nM purified PadR, as previously described (32). DNase I digestions were optimized. Briefly, 100-μl reaction mixtures included radioactive DNA probes incubated for 1 min at 37°C with 0.5 U of DNase I. DNase I digestion was stopped by addition of a solution containing 200 mM NaCl, 20 mM EDTA, 10 g/liter SDS, and 10 mg/ml salmon sperm DNA. DNA products were purified by ethanol precipitation and resuspended in 10 μl of TE (10 mM Tris-HCl, 1 mM EDTA) buffer. Samples were mixed 1:1 with gel sequencing loading buffer and then resolved in a denaturing 6% (wt/vol) polyacrylamide-urea electrophoresis gel and visualized by autoradiography. Sequencing reactions were performed with corresponding primers for each strand, using a CycleReader DNA sequencing kit (MBI-Fermentas). These reactions were run adjacent to their respective DNase I footprinting samples.

EMSA. The 234-bp *padC* promoter DNA probe P1 used for DNase I footprinting assays was also used for EMSA. Matching experiments were performed with modified *padC* promoters generated with the appropriate primers listed in Table 2. PCR products were purified using a QIAquick PCR purification kit. Standard EMSA was performed as described previously (32). Briefly, purified native or modified PadR was incubated for 20 min at 28°C in 15 μl binding buffer containing 0.2 nM DNA probe, 10 mM Tris-HCl, pH 7.8, 5% (vol/vol) glycerol, 0.2 mM EDTA, 2.5 mM $MgCl_2$, 50 mM KCl, 2 mM dithiothreitol (DTT), 2.5 μg/ml bovine serum albumin (BSA), and 2.5 μg/ml salmon sperm DNA.

The samples were resolved in 5% (wt/vol) polyacrylamide gels and analyzed by autoradiography. To test the effects of phenolic acids on PadR-*padC* promoter DNA binding, PadR was preincubated with 1 mM *p*-coumaric, ferulic, or *o*-coumaric acid in 15 μl of binding buffer for 5 min at room temperature. *o*-Coumaric acid, an isomer of *p*-coumaric acid unable to induce the expression of *padC* (32), was used as a negative control at 1 mM. The probe was then added to the above mixture and incubated for 20 min at 28°C before loading onto a polyacrylamide gel.

Production of modified *padC* promoter probes. All probes used in this study were PCR amplified from *B. subtilis* 168 genomic DNA by use of three different primers: an internal primer carrying the desired modification and two external primers (Table 2). The external primers were previously labeled with T4 poly-

TABLE 1. Plasmids and bacterial strains

Plasmid or strain	Genotype and/or relevant feature(s)	Source or reference
Plasmids		
pET28a+	Kan^r; vector for overexpression of His-tagged proteins using T7 bacteriophage promoter	Novagen
pER	pET28a+ containing *padR* between BspHI and XhoI sites to overproduce PadR with His_6 tag	32
pERM (1-16)	pET28a+ containing modified *padR* genes	This work (Fig. 5B)
pJM783	Amp^r Cm^r; integrative vector used to construct the *lacZ* transcriptional fusion F1	30
pHT315	Ery^r Amp^r	3
pHR	pHT315 containing *padR* between XbaI and PstI sites	This work (Fig. 4A)
pHRM (1-16)	pHR containing modified *padR* genes between BseRI and PstI sites	This work (Fig. 4A)
Strains		
B. subtilis strains		
168	*trpC2*	Institut Pasteur, France
168 Δ*padR*	*trpC2* Spec^r Δ*padR* mutant of BS168	32
783F1	*trpC2* Amp^r Cm^r; carries the F1 *padC*::*lacZ* fusion	32
783F1 Δ*padR*	*trpC2* Spec^r Δ*padR* Amp^r Cm^r; contains the F1 *padC*::*lacZ* fusion	This work (Fig. 1)
783F1 Δ*padR*/pHRM	*trpC2* Spec^r Δ*padR* Amp^r Cm^r; contains the F1 *padC*::*lacZ* fusion and pHRM plasmid	This work (Fig. 1)
168 Δ*padR*/pHRM	*trpC2* Spec^r Δ*padR* mutant containing pHRM plasmid	This work (Fig. 4B)
E. coli strains		
TG1	*supE hsd*Δ*5thi* Δ(*lac-proAB*) F′ *traD36 proAB*$^+$ *lacI*^{q} *lacZ*ΔM15	Invitrogen
TG1/pHR	Amp^r; carries plasmid pHR	This work (Fig. 4A)
TG1/pHRM	Amp^r; carries plasmid pHRM	This work (Fig. 4A)
BL21(DE3) Star	*pThsdS*$_B$(r_B^- m_B^-) *gal dcm* (DE3)	Invitrogen
BL21/pER	BL21(DE3) Star carrying plasmid pER	This work (Fig. 5B)
BL21/pERM (1-16)	BL21(DE3) Star carrying plasmid pERM	This work (Fig. 5B)

nucleotide kinase (Invitrogen) in the presence of [γ-^{32}P]ATP (Perkin-Elmer). The PCR consisted of two steps. First, the internal primer was used together with the appropriate external primer to introduce the modification, and second, the resulting product was used as a primer together with the second external primer (Table 2) to obtain the final product. Nonlabeled corresponding modified sequences were verified by sequencing (Cogenic).

Random mutagenesis of *padR* by error-prone PCR and screening for modified *padR* genes of interest. Random mutagenesis of *padR* was carried out *in vitro* with a GeneMorph II random mutagenesis kit (Stratagene). PCR amplification was performed in a 50-μl reaction mixture containing 100 ng of genomic DNA extracted from *B. subtilis* 168 cells, 2.5 U of Mutazyme II DNA polymerase, a 40 mM deoxynucleoside triphosphate (dNTP) mix, and 250 ng/μl (each) of BSR5 and BSR101 primers (Table 2). The reaction conditions were designed to achieve 0 to 4 mutations per kb of DNA. To avoid any modification to the unknown promoter region of *padR* and to facilitate cloning, the native BseRI restriction site was used with the PstI restriction site to replace the native *padR* gene with the mutated *padR* genes. Error-prone PCR products were purified, digested by the BseRI and PstI enzymes, and cloned into plasmid pHR. After ligation, the reaction mixtures containing the resulting pHRM plasmids were transformed into *E. coli* TG1. About 5,000 colonies were obtained. A three-step procedure was used to efficiently screen *padR* mutant genes of interest (Fig. 1). Two hundred colonies were analyzed individually by PCR amplification to verify the presence of a *padR* amplicon with the expected size. Positive colonies were used in a second step consisting of gradient SDS-polyacrylamide gels to select cultures producing a modified PadR protein (PadRM). pHRM plasmids from these cultures were transformed individually into the *B. subtilis* 783F1 Δ*padR* reporter strain (see below) to screen modified *padR* genes of interest with the LacZ phenotype. Modified *padR* genes of interest were sequenced to identify mutated nucleotides. These plasmids were then transformed into a *B. subtilis* Δ*padR* strain. Comparisons of strains with plasmids to control strains were made by analysis of the LacZ phenotype and phenolic acid decarboxylase (PAD) activities.

Construction of *B. subtilis* 168 reporter strains to screen modified *padR* genes of interest. *B. subtilis* strain 783F1 Δ*padR* (Fig. 1) was obtained by transforming strain 783F1 with chromosomal DNA from a *B. subtilis* Δ*padR* strain (32) and selecting LacZ$^+$ colonies (blue) on LB agar plates containing X-Gal (5-bromo-4-chloro-3-indolyl-β-D-galactopyranoside) supplemented with spectinomycin. *B. subtilis* 783F1 Δ*padR* did not display PAD activity with (inducing [I] conditions) or without (noninducing [NI] conditions) ferulic acid. The absence of PAD activity is due to the separation of the functional *padC* promoter from the *padC* gene by integration of a pJM783 vector containing a truncated, nonfunctional *padC* promoter (32). The constitutive LacZ$^+$ phenotype results from the deletion of *padR* by replacement with the *speR* cassette. The wild-type *padR* gene in plasmid pHR was replaced by different modified *padR* genes to generate the pHRM plasmids. These plasmids were transformed into strain 783F1 Δ*padR* (Fig. 1). The transformation mixture was poured onto LB agar plates supplemented with erythromycin and X-Gal and with (I conditions) or without (NI conditions) ferulic acid. The selection of colonies was based on LacZ reporter phenotypes, which we were able to classify into five discernible intensities ranging in color from blue to white. As a reference, we used strain 783F1 Δ*padR*. For instance, 783F1 Δ*padR* yields a deep-blue LacZ reporter phenotype, or LacZ 5; this strain complemented with native *padR* on LB medium without ferulic acid yields a white LacZ phenotype, or LacZ 0; and this strain on LB medium with ferulic acid yields a lighter blue color, or LacZ 4. LacZ level 2 and 3 colonies were colonies initially formed with at least two contiguous bacteria. However, after reisolation, these displayed LacZ levels 0 and 2 and then levels 2 and 4, respectively.

Overexpression and purification of native PadRs and PadRMs. Expression and purification of PadR proteins were performed as described previously (32). The PadR and modified PadR (PadRM) coding regions were PCR amplified with the BSR1 and BSR2 primers to replace the TAA stop codon with an XhoI restriction site. The amplified DNA fragment was cloned into the pET28a+ vector by NcoI and XhoI digestion, generating the plasmids pER and pERM. Expression of pER and pERM in *E. coli* BL21(DE3) cells induced with IPTG (isopropyl-β-D-thiogalactopyranoside) produced PadR fusion proteins containing a His_6 tag at the C-terminal end. Recombinant PadR and PadRM proteins were purified from *E. coli* BL21(DE3) cell extracts by elution from a 0.5-ml nickel-nitrilotriacetic acid (Ni-NTA) column (Qiagen) according to the manufacturer's guidelines. Purified protein samples were stored at −25°C.

Cell extracts, assay for PAD activity, and protein gel electrophoresis. Wild-type and mutant *B. subtilis* 168 strains grown in LB medium were harvested and disrupted using a Z Plus series cell disrupter (Constant system) (15). PAD activity in cell extracts was measured by monitoring the kinetics of absorption peaks by UV spectrophotometry (6). Protein concentrations were determined using a Bio-Rad protein assay kit with BSA as the standard. Protein extracts were routinely resolved in a 12% (wt/vol) denaturing SDS-PAGE gel as previously described (14). To verify PadRM protein expression in crude extracts from

TABLE 2. Primers used for this study

Primer use and name	Sequence (5′→3′)[a]	Site created/modified
Cloning of *padR* into pET28a+		
BSR1	GACTCATGAGAGTATTAAAATACGCC	BspHI
BSR2	GCTCTCGAGATCCTTATCTATCATAG	XhoI
Cloning of *padR* into pHT315		
BSR3	TACGTCTAGAGACAGGATTATGTACTGACT	XbaI
BSR4	AAGCTGCAGGATCGACATTGAA	PstI
Random mutagenesis of *padR* by error-prone PCR		
BSR5	ATGCTGCAGATTATCGCTAACGGTGCC	PstI
BSR101	ATGAGAGTATTAAAATACGCC	BseRI (native)
Production of *padC*::*lacZ* fusions		
BSDF1	CCAGAATTCACGGCAAGTCAGCAAGCCGT	EcoRI
BSDFR	TCAGGATCCGATAAAGTTTTCCATCTTACAC	BamHI
Sequencing of *padR* mutants		
BSR6	TCGGATACCTTCTGACAA	
Probes for DNA binding		
BSD1	CAAAGCTAGCTTCAGACAAGG	
BSD2	CACTTTAACACCATTGCAG	
BSD4	ATGTAACTATTTACATGTTCAC	
BSD5	GCAATGGTGTTAAAGTGAACATGT	
BSD5IR1 (forward)	GCAATGGTGTTAAAGTGAACΔAAATAGTTACATGATTTTTTC	ΔIR1 (ATGT)
BSD5IR2 (forward)	GCAATGGTGTTAAAGTGAACATGTAAATAGTTΔGATTTTTTC TGAAGGTGAGGTG	ΔIR2 (ACAT)
BSD5IR12 (forward)	GCAATGGTGTTAAAGTGAACΔAAATAGTTΔGATTTTTTC	ΔIR1, ΔIR2
BSD6	ACATGTTCACTTTAACACCATTGC	
BSD8 (reverse)	GAATCATCTCAGTCCCAGGCTTG	

[a] Underlined nucleotides correspond to restriction sites for the enzymes given in the right column.

recombinant *E. coli* strains, 8 to 15% (wt/vol) gradient SDS-PAGE (18-cm by 18-cm gel) was run for 5 h at 110 V.

RESULTS

Identification of PadR binding site for the *padC* promoter. In the absence of phenolic acid (nonstress, noninduced conditions), PadR binds to the *padC* (*yveFG-padC*) promoter, thereby repressing its expression. Our previous studies showed a consensus inverted repeat DNA sequence (ATGT-8N-ACAT) in the *padC* (*yveFG-padC*) promoter that is found in the promoters of *padC* or *padA* genes in bacteria displaying the PASR (32) and has a suspected interaction with PadR (32). To identify the binding sites of PadR for the *padC* promoter, DNase I footprinting experiments were performed. For these assays, protection of a radioactively labeled 234-bp fragment extending from nucleotides (nt) −97 to +137 relative to the +1 start of transcription of the *padC* promoter was observed in the presence of different concentrations of purified PadR (Fig. 2). Consistent results were obtained for the two DNA strands (Fig. 2A and B). A PadR concentration of 0.1 nM did not result in detectable protection; however, we did observe DNA protection at a PadR concentration of 1 nM. At this concentration of PadR, previous gel shift assays demonstrated two specific shifted bands for the probe in EMSAs (32). This 42-bp region includes the previously supposed consensus 16-bp inverted repeat ATGT-8N-ACAT (IR1-2) (Fig. 2C). In addition to the IR1-2 sequence, there exists a degenerate IR1-2 sequence (GTGT-8N-ACAT), named dIR1-2bis, that contains an ACAT pattern overlapping the AT nucleotides (ATGT) in the IR1 region (Fig. 2C). Like the IR1 region, the dIR1 region is followed by a stretch of 3 adenosines. The dIR1-2bis/IR1-2 pattern (which includes nucleotides at positions −15 to +15 relative to the *padC* +1 start of transcription) resided within the region protected by PadR at 1 nM (from position −20 to position +22) (Fig. 3A). When 10 nM PadR was used, a concentration where a single shift was found by EMSA (32), this protected region could be extended upstream to encompass the −10 and −35 promoter boxes and to roughly 20 nt downstream of the dIR1-2bis region (Fig. 2C).

EMSA with PadR and mutated *padC* promoters. Since we showed that the sequence containing the dIR1-2bis/IR1-2 pattern resided within the region protected by PadR (Fig. 2), our next objective was to determine the functional specificity of this binding. PCR was used to generate a probe containing the entire 234-bp native promoter and seven other mutated promoter probes (Fig. 3B). These probes were then tested for binding to PadR (Fig. 3C and D). With the P1 fragment, which contains the entire promoter region and 1 nM PadR, two specific complexes, C1 and C2, were found, accounting for two operator sites. Nevertheless, C3, a high-molecular-mass complex, was found with this probe at 10 nM PadR. This binding may be accounted for by additional lower-affinity or less specific bindings of PadR proteins to the region extending upstream of the −35 box (Fig. 2). This finding corroborates the results obtained after footprinting assays with 10 nM PadR, where we found that the protected region extends to the −40

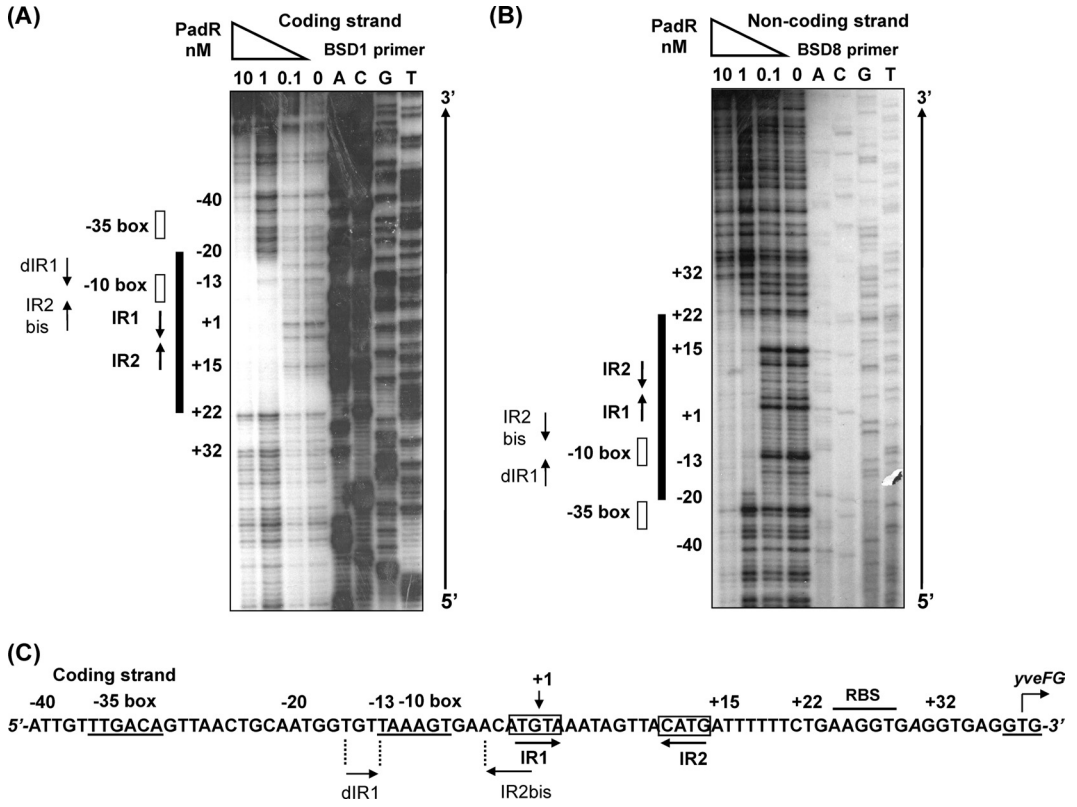

FIG. 2. *padC* (*yveFG-padC*) promoter DNA protection with PadR. Purified PadR was incubated with a 234-bp single-end-labeled *padC* promoter DNA probe. The reaction mixtures contained a 5′-[γ-^{32}P]ATP-labeled coding strand (BSD1 primer) (A) or noncoding strand (BSD8 primer) (B) that was digested by DNase I. The reaction mixtures were run adjacent to corresponding DNA sequencing reaction mixtures (ACGT). (C) *padC* promoter coding strand sequence, with nt positions, +1 transcription start site, and −35 and −10 boxes for the *padC* promoter operon indicated, as well as the GTG start codon of *yveFG* (32). RBS, ribosome binding site. IR1, IR2, dIR1, and IR2bis are inverted repeat sequences for PadR.

position (Fig. 2). This suggests the existence of a possible additional, less specific binding site(s) of PadR, even though the IR1-IR2 pattern (or a degenerate version) is not observed within this sequence.

The presence of two inverted repeat dyads in the promoter and of two complexes, C1 and C2, in the presence of 1 nM PadR corresponds to a modified overlapping binding model, as described for the Fur repressor binding site involved in iron uptake in *E. coli* (21). These findings are reinforced by the fact that we demonstrated that in *B. subtilis* 168, PadR easily forms dimers at low concentrations of the cross-linking reagent glutaraldehyde (0.1% [vol/vol]) (see the supplemental material). Moreover, the 42-nt length of the *padC* promoter protected region with 1 nM PadR is sufficient to bind two PadR dimers. This is supported by many studies that report DNA regions protected by one dimer repressor that extend over 19 to 27 nt (16, 21). Binding of PadR at 1 nM to the P1, P4, and P5 probes, which contained the entire dIR1-2/IR1-2 sequence, produced C1 and C2 complexes. Using the P3 fragment, which contained only dIR1-2bis/IR1 and not the IR2 sequence, C1 and C2 complexes were detected, suggesting that this region is sufficient to bind to two PadR molecules. The low-intensity C1 band observed with the P5ΔIR1 probe probably resulted from binding to the IR2 sequence, since this C1 complex was not observed with the P5ΔIR1-2 probe.

Moreover, the C2 complex did not form when the sequences encompassing IR1 and half of IR2bis (AC) (probes P2, P5ΔIR1, and P5ΔIR1-2) were absent. Experiments with the P2 probe indicated that the dIR1 (GTGT) sequence, in addition to any upstream sequences, was not capable of binding to PadR at 1 nM but produced the C3 complex in the presence of 10 nM PadR. On the other hand, C1 and C2 complexes were present with the P4 fragment (the probe containing dIR1-2bis/IR1-2), indicating that the sequence downstream of IR2 is not necessary for C1 and C2 complex formation. However, this sequence might produce a lower-affinity or less specific binding participating in the formation of the less specific C3 complex, since it was partially protected at 10 nM PadR. Taken together, these findings indicate that the dIR1-2bis/IR1 sequence is mainly responsible for the interaction with PadR. A C2 complex was detected with the P5ΔIR2 probe, indicating that this probe is able to bind *in vitro* to two dimers of PadR, as does the P1 probe containing the IR2 sequence. It is likely that the IR1 sequence is sufficient to bind *in vitro* to a PadR dimer. Further comparison of these EMSA results with those obtained with P5ΔIR1 and P5ΔIR1-2 fragments indicates that IR2 (probe P5ΔIR1) contributes to PadR binding. Indeed, use of IR2 produced a significant amount of C1 complex, corresponding to binding of one PadR dimer. The C1 complex was not ob-

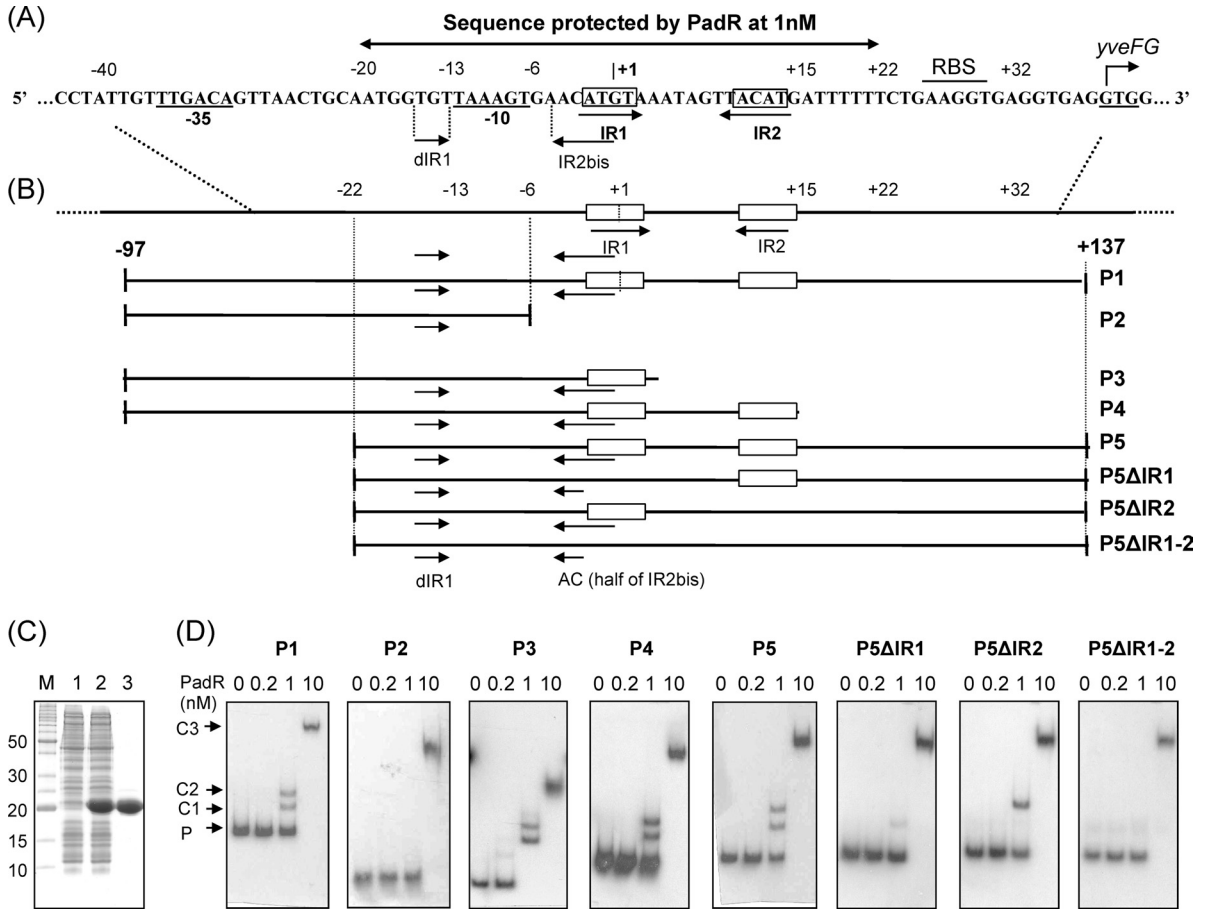

FIG. 3. EMSA for PadR with native and modified *padC* promoters. (A) *padC* promoter DNA sequence indicating nt positions from the +1 transcription start site, −35 and −10 boxes, and IR1-IR2 and dIR1-2bis, the inverted repeat sequences that form the dIR1-2bis/IR1-2 pattern. The start codon (GTG) of *yveFG*, a nonfunctional gene cotranscribed with *padC* (32), is indicated. (B) Map of native (P1) and modified (P2 to P5 and P5 derivatives) *padC* promoters used in EMSA. (C) SDS-PAGE of protein extracts containing purified PadR used in EMSA. Lane M, molecular mass standard; lanes 1 and 2, crude extracts from *E. coli* BL21 and *E. coli* BL21/pER, respectively; lane 3, purified PadR. (D) EMSAs with native and modified *padC* promoters (0.2 nM). PadR was used in EMSAs at concentrations ranging from 0 to 10 nM. A concentration of 1 nM PadR gave specific binding (C1 and C2 complexes), while 10 nM PadR gave unspecific binding (C3 complex). P, unbound probe. For panel D, all PAGE experiments were run under the same conditions, and the fact that the probes and the complexes in the different panels are not aligned horizontally results from the different sizes of the probes (P1, 234 bp; P2, 91 bp; P3, 102 bp; P4, 112 bp; P5, 159 bp; P5ΔIR1 and P5ΔIR2, 155 bp; and P5ΔIR1-2, 151 bp).

served when the P5ΔIR1-2 probe was incubated with IR2-null sequences.

Identification of single amino acid substitutions modifying the functionality of PadR. Random mutagenesis of *padR* and construction of an appropriate recipient and reporter *B. subtilis* strain, strain 783F1 Δ*padR*, were performed to identify which amino acid residue(s) is important for PadR structure-function. To screen modified *padR* genes of interest, we employed the strategy schematized in Fig. 1. Two hundred colonies, from 5,000 originally isolated after transformation of *E. coli*, were analyzed individually by PCR amplification to verify the presence of a *padR* amplicon of the expected size. Seventy amplicons showed the expected size. Protein extracts from these clones were analyzed by SDS-PAGE. Among them, only 32 strains exhibited a PadR protein with the expected size. Plasmid DNAs from these strains were transformed into strain 783F1 Δ*padR*. Transformed colonies were selected on LB–X-Gal medium with (I conditions) and without (NI conditions) ferulic acid by comparing their LacZ phenotype color intensities (from white [LacZ 0] to deep blue [LacZ 5]) to those of control strains 783F1 and 783F1 Δ*padR* as described above. Mutant colonies with a LacZ phenotype different from that of 783F1 Δ*padR* complemented with the native *padR* gene on LB medium, with or without ferulic acid, were selected. The corresponding mutant *padR* genes were then sequenced and translated to identify amino acid residue changes. Eleven putative mutants initially displayed a LacZ color phenotype of 3 to 5. During their propagation, many changed their LacZ color phenotype to level 4, which was obtained with wild-type PadR. Further sequence investigations showed that these putative mutants contained native *padR*, and therefore these clones were excluded from further analysis. Two mutants displaying a stable LacZ level of 5 under I or NI conditions had double mutations, at residues 46 to 128 and residues 61 to 128. These were not analyzed further. The remaining 19 mutants (M clones) were classified into three groups (Fig. 4B). Group 1

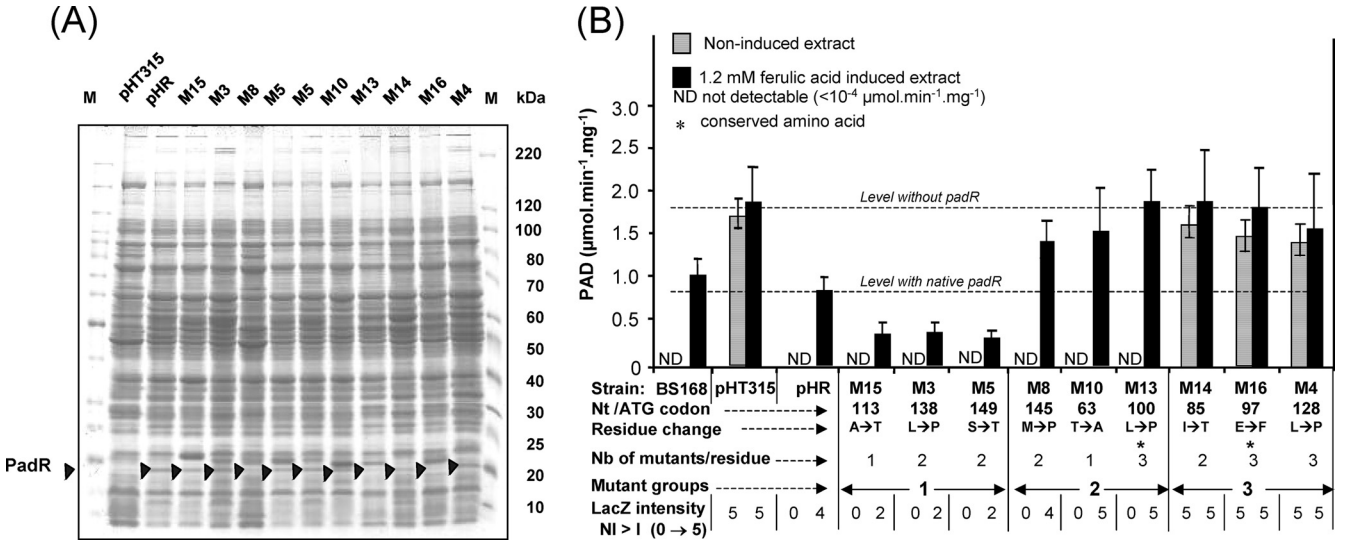

FIG. 4. (A) SDS-PAGE analysis of modified PadR (black triangles) expressed in *E. coli* strains. (B) PAD activities (μmol min^{-1} mg^{-1}; data are averages for three experiments) in mutant strains complemented with native *padR* (pHR) or modified *padR* genes (pHRM). Cultures were induced or not with 1 mM ferulic acid for 20 min before harvesting and disrupting the cells. *B. subtilis* 168, wild-type strain; pHT315, 168 Δ*padR* mutant transformed with pHT315 (without *padR*); pHR, 168 Δ*padR* mutant complemented with native *padR*; M15 to M4, 168 Δ*padR* mutants complemented with modified *padR*. These mutants form three groups based on PAD activity compared to that with native *padR* (pHR).

consisted of five mutants giving white colonies (LacZ 0) under NI conditions and a LacZ level of 2 under I conditions (which was lower than that of control strain 783F1). Sequencing of *padR* revealed modifications at residues 113, 138, and 149 for clones M15, M3, and M5, respectively. Group 2 contained six PadRMs giving white colonies (LacZ 0) under NI conditions and blue colonies (LacZ 5) under I conditions. Sequencing of *padR* revealed modifications at residues 145, 63, and 100 for clones M8, M10, and M13, respectively. Group 3 contained eight PadRMs with a LacZ level of 5 under both NI and I conditions, which is equivalent to the level for 783F1 Δ*padR* (without *padR*). Sequencing revealed mutations at residues 85, 97, and 128 for clones M14, M16, and M4, respectively. Substitutions of nine different residues were found to modify the function of PadR.

The plasmids containing the 9 modified *padR* genes were transformed into the recipient Δ*padR* strain with a functional *padC* gene (Fig. 1) in order to compare PAD activities (under I and NI conditions) with those observed for native PadR (Fig. 4B). For all PadRMs, the LacZ phenotype correlated well with the PAD activity. Group 1 mutants displayed no detectable activity under NI conditions and a PAD activity 2- to 2.5-fold lower than that of the pHR strain under I conditions. These results show that modified PadRMs maintained their repressor function but were not completely inactivated by ferulic acid. Repressor function was also retained in group 2 mutants, but PAD activity in induced cultures was increased 2-fold compared to that observed in controls (Fig. 4B). Finally, group 3 mutants under NI conditions displayed a PAD activity fairly identical to that obtained under I conditions. These findings indicate that PadRMs of this group are not functional. We then verified that the His-tagged native PadR protein, whose gene was cloned into vector pHT315 and expressed in strain 168 Δ*padR*, displayed the same function as the native nontagged PadR protein (data not shown), demonstrating that the phenotypes of mutants were the consequences of the single amino acid changes. Interesting results were obtained for two lysine-to-proline substitutions, in M4 (position 128) and M3 (position 138), both of which affect the coiled-coil motif. The M4 substitution (which affects the middle of the predicted coiled-coil motif) produced a nonfunctional PadRM4, while the M3 mutation (which affects the tail end of the motif) led to a reduction of PAD activity only under induced conditions. These results demonstrate that replacement of a lysine residue at the center of a coiled-coil motif by a proline leads to a high degree of disorder of the secondary structure of PadR, while the same substitution in the extremity of the coiled-coil motif has less of an influence on PadR protein structure and function.

Interaction of PadRMs with native *padC* promoters. To further characterize PadR-*padC* sites of interaction, one modified *padR* gene representative of each of our three groups was cloned into the vector pET28a+ and expressed in *E. coli* BL21 to produce the corresponding PadRMs (Fig. 5A). The levels of interaction between these purified PadRMs at different concentrations were analyzed by EMSA with the *padC* promoter probes at 0.2 nM (Fig. 5B). The *padC* promoter required concentrations ranging from 0.5 (not tested in the experiments shown in Fig. 3D) to 1 nM native PadR to yield complexes C1 and C2. C1 and C2 correspond to binding of the probe to one and two PadR dimers, respectively. Increasing the concentration of PadR from 2 to 5 nM produced new complexes with higher molecular weights that could correspond to additional bound PadR dimers, probably to the upstream region of the −35 box and possibly to the downstream region of IR2. This point was previously discussed in the analysis of the C3 complex and was incorporated into our model (Fig. 5C). In this case, the C3 complex corresponds to the saturation of the probe by PadR dimers, which was observed when incubation mixtures included 5 nM (Fig. 5B) and 10 nM (Fig. 3D) PadR.

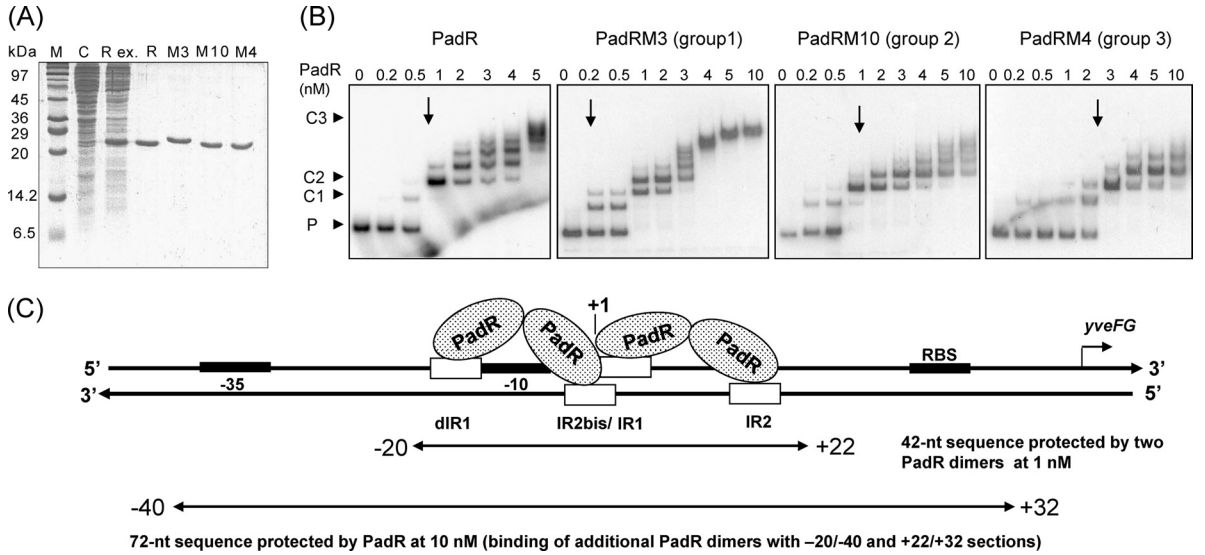

FIG. 5. (A) SDS-PAGE of native (R) and modified (M3, M10, and M4) His_6-tagged PadRs produced in *E. coli* and used in EMSA. M, molecular mass standard; C, control *E. coli* strain with pET28a+; Rex, crude extract of native PadR. The same types of extracts were produced to purify the native protein and M3, M10, and M4, shown in the corresponding lanes. (B) EMSAs of native and modified PadRs (M3, M10, and M4), representing the three groups based on PAD activity with the native *padC* promoter probe at 0.2 nM (see Fig. 4). P, promoter DNA probe without PadR. C1 and C2 indicate specific complexes formed between the DNA probe and PadR. C3 results from additional low-affinity or less specific binding. Arrows indicate the concentrations at which the specific complexes C1 and C2 are observed. (C) Model for PadR dimer binding to *padC* (*yveFG*) promoter. The protected sequence was deduced from the results presented in Fig. 2. One dimer binds to dIR1 and the complementary sequence of IR2bis, and the second dimer binds to IR1 and the complementary sequence of IR2.

For PadRM3 (group 1), C1 and C2 complexes were observed at 0.2 nM, and saturation of the probe was obtained at approximately 4 nM. These results indicate that the PadRM3 group displays a higher affinity for the probe and corroborate the LacZ phenotype and PAD activity of these mutants as shown in Fig. 4B. For PadRM10 (group 2), C1 and C2 complexes were obtained at 0.5 to 1 nM, similar to the results obtained for native PadR. These findings may explain the absence of detectable PAD activity with this group of PadR mutants under NI conditions, identical to the case for native PadR. Nevertheless, increasing the concentration of PadRM10 did not produce complexes of significantly higher molecular mass, and C3 was not detected in the presence of 10 nM PadR. These results reflect a reduced capacity of PadRM10 to bind to the *padC* promoter and correlate with a higher PAD activity under ferulic acid-induced conditions (Fig. 4B). For PadRM4 (group 3), the C1 complex was detected by EMSA at 0.2 to 0.5 nM PadR, but the C2 complex was detected only when the PadR concentration was higher than 2 nM. Additionally, as observed with PadRM10, increasing the concentration to 10 nM PadRM4 did not produce the C3 complex. Taken together, these findings indicate that the lysine-to-proline substitution at position 128 in PadRM4 reduces the capacity to produce the C2 complex and causes an inability to produce the C3 complex. This substitution, which occurs at the center of the putative coiled-coil motif, may modify the dimer structure and alter the recognition of at least one of the two binding sites of the *padC* promoter. This correlates with the inability of PadRM4 to repress the expression of *padC* under noninduced conditions.

Effects of phenolic acids and $MgCl_2$ on PadRM binding to the *padC* promoter. It was previously shown that phenolic acids capable of inducing the PASR were able to abolish PadR binding to the *padC* promoter (32). In order to test whether single-residue substitutions in PadRMs could modify the response to phenolic acids, EMSAs with native PadR, PadRMs, and the *padC* promoter were performed in the presence or absence of $MgCl_2$ and with or without preincubation with phenolic acids (Fig. 6), as previously described (32). For an effective comparison of our findings, we used the results obtained with our PadR-*padC* interaction site studies (Fig. 5) to choose for each PadRM the concentration yielding the specific complexes C1 and C2. Specific emphasis was placed on PadRMs yielding a high concentration of C2, which corresponds to the binding of two PadR dimers with the probe. For native PadR, binding was not altered by phenolic acids in the presence of $MgCl_2$ but was abolished in the absence of $MgCl_2$ with 2 or 4 mM *p*-coumaric or ferulic acid, two inducers of the PASR (Fig. 6), but not with *o*-coumaric acid, a noninducer of the PASR. Therefore, the absence of the C1 complex from the relevant lane indicates that the inactivation of PadR by phenolic acid *in vitro* results in suppression of binding with the two sites formed by the dIR1-2/IR1-2 pattern. Furthermore, *o*-coumaric acid, an isomer of *p*-coumaric acid, was not able to abolish the binding. For PadRM3 (group 1) at a concentration of 0.2 nM, we detected only a partial release of the probe with *p*-coumaric (P2 and P3) and ferulic (F2 and F3) acids in the absence of $MgCl_2$. In addition, we detected no probe release under the same conditions for incubation with *o*-coumaric acid. The absence of a complete release of the probe in the absence of $MgCl_2$ corroborates our finding that PadRM3 is inactivated by phenolic acids *in vivo* to a lesser extent than native PadR (Fig. 4B). A similar yet more robust liberation of the probe was noted for PadRM10 (group 2) at 1 nM, which was unexpected because this PadRM is inactivated by phenolic acids to a

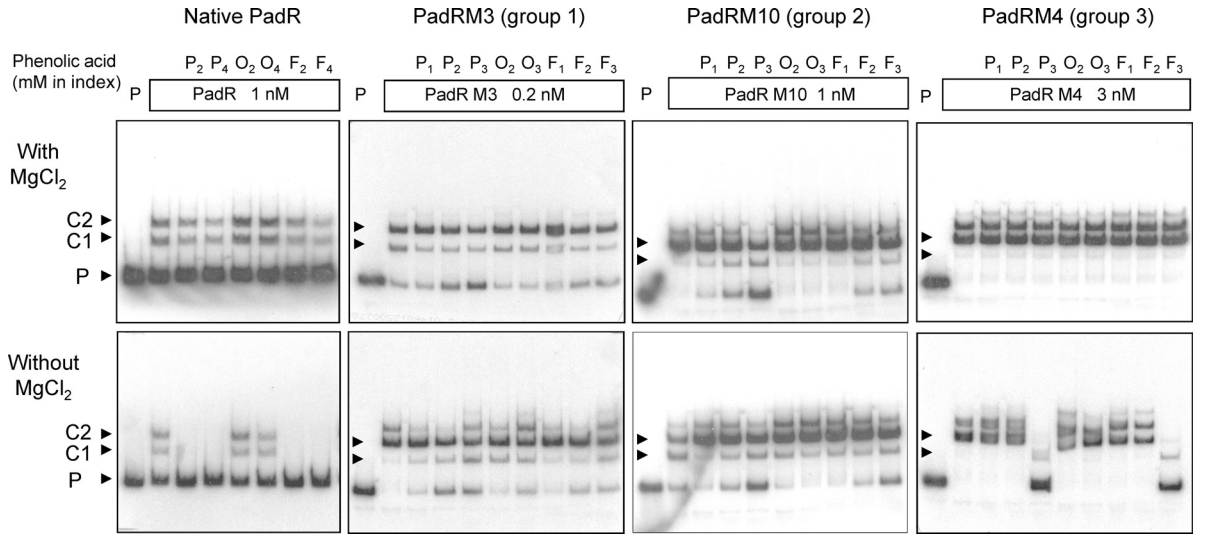

FIG. 6. EMSAs of native and modified His_6-tagged PadRs M3, M10, and M4, representative of the three groups based on PAD activity with the native *padC* promoter at 0.2 nM (see Fig. 3B), in the presence or absence of $MgCl_2$ or phenolic acids. P_n, *p*-coumaric acid; O_n, *o*-coumaric acid (isomer of *p*-coumaric acid unable to induce the PASR); F_n, ferulic acid; P, *padC* promoter probe. The concentration of each PadR protein was chosen to obtain the two specific complexes, C1 and C2, with the *padC* promoter (see Fig. 5).

greater extent *in vivo* than native PadR. Lastly, PadRM4 (group 3) at 3 nM (the concentration giving a C2 major complex) demonstrated no significant changes in EMSA with addition of phenolic acid in the presence of $MgCl_2$. However, we observed a release of the probe when PadRM4 was incubated with PASR acid inducers (P3 and F3) in the absence of $MgCl_2$. This release was comparable to that observed with native PadR, except for the apparition of a low-intensity band corresponding to the size of the C1 complex. It is noteworthy that the *in vivo* findings do not correlate strictly with our EMSA results. Nevertheless, our data suggest that the residues mutated in PadRM3 and PadRM10 might be involved in the inactivation mechanism induced by phenolic acids.

Comparison of PadR and AphA secondary structures. Multiple alignments of seven PadRs involved in the PASR were performed to identify conserved nucleotides, amino acid residues in the putative coiled-coil leucine zipper motif (predicted with COILS software [24]), and the conserved N- and C-terminal sequences (Fig. 7A). The positions of the mutations within this sequence were analyzed. Since we used the native BseRI restriction site at residue 39 for cloning of all mutated *padR* genes, there was no mutation produced upstream of residue 39. Therefore, except for three mutants (one M10 and two M14 mutants), all other mutants contained mutations from residue 97 (M16) to residue 149 (M5), which encompass the putative coiled-coil leucine zipper motif that is considered to be involved in the dimerization of regulator proteins, notably those belonging to the GntR superfamily, of which PadR is a member. This is in accordance with cross-linking (see the supplemental data) and EMSA results indicating that PadR dimerization is required for its interaction with the *padC* promoter.

The hypothetical secondary structure of PadR predicted by the PSIPRED program (26) shows high similarities in structural elements with the secondary structure of AphA determined from its crystal structure (Fig. 7B) (11). The PadR hypothetical coiled-coil domain, determined by the use of COILS software (24), spans amino acids 118 to 140 (Fig. 7A).

DISCUSSION

In this work, we characterized the *padC* promoter region to which PadR binds in *B. subtilis* 168 when it is not exposed to phenolic acids, and thereby when expression of *padC* is completely repressed. We showed that the binding region of the *padC* gene contains a consensus IR1-2 inverted repeat, ATGT-8N-ACAT, and an overlapping upstream degenerate repetitive sequence, dIR1-2bis (gTGT-8N-ACAT). This pattern, named dIR1-2bis/IR1-2, which extends over 42 nt, corresponds to the sole region protected by 1 nM PadR. Footprinting and EMSA analyses revealed an extension of the protected region covering the upstream −35 box and a section from positions +22 to +32 (where +1 refers to the transcription initiation site) that could be responsible for additional low-affinity or less specific binding of PadR dimers with increasing concentrations of PadR from 2 to 10 nM (Fig. 5B and C). These additional binding sites could reinforce repression of the promoter under NI conditions. The length of the protected region with 1 nM PadR allows, depending on the concentration of PadR in EMSAs, the binding of one or two PadR dimers, which produces two complexes in EMSA, i.e., C1 and C2. As mentioned previously, IR1-2 is found in the *padC* (or *padA*) promoter in all bacteria displaying the PASR. While the dIR1-2bis sequence is also found in the *padA* promoter in *L. plantarum* (14), which does not form an operon with *padR*, dIR1-2bis is not found in the promoter of the *P. pentosaceus padA* gene, which does form a *padAR* operon with *padR* (7). We speculate that to repress *padAR* expression in *P. pentosaceus*, the binding of PadR to the *padAR* promoter may involve only one PadR dimer and may be reduced compared to that observed in *B. subtilis* 168 or *L. plantarum*. For *B. subtilis* 168 and *L. plantarum*, it is reasonable to think that under NI conditions *in vivo*,

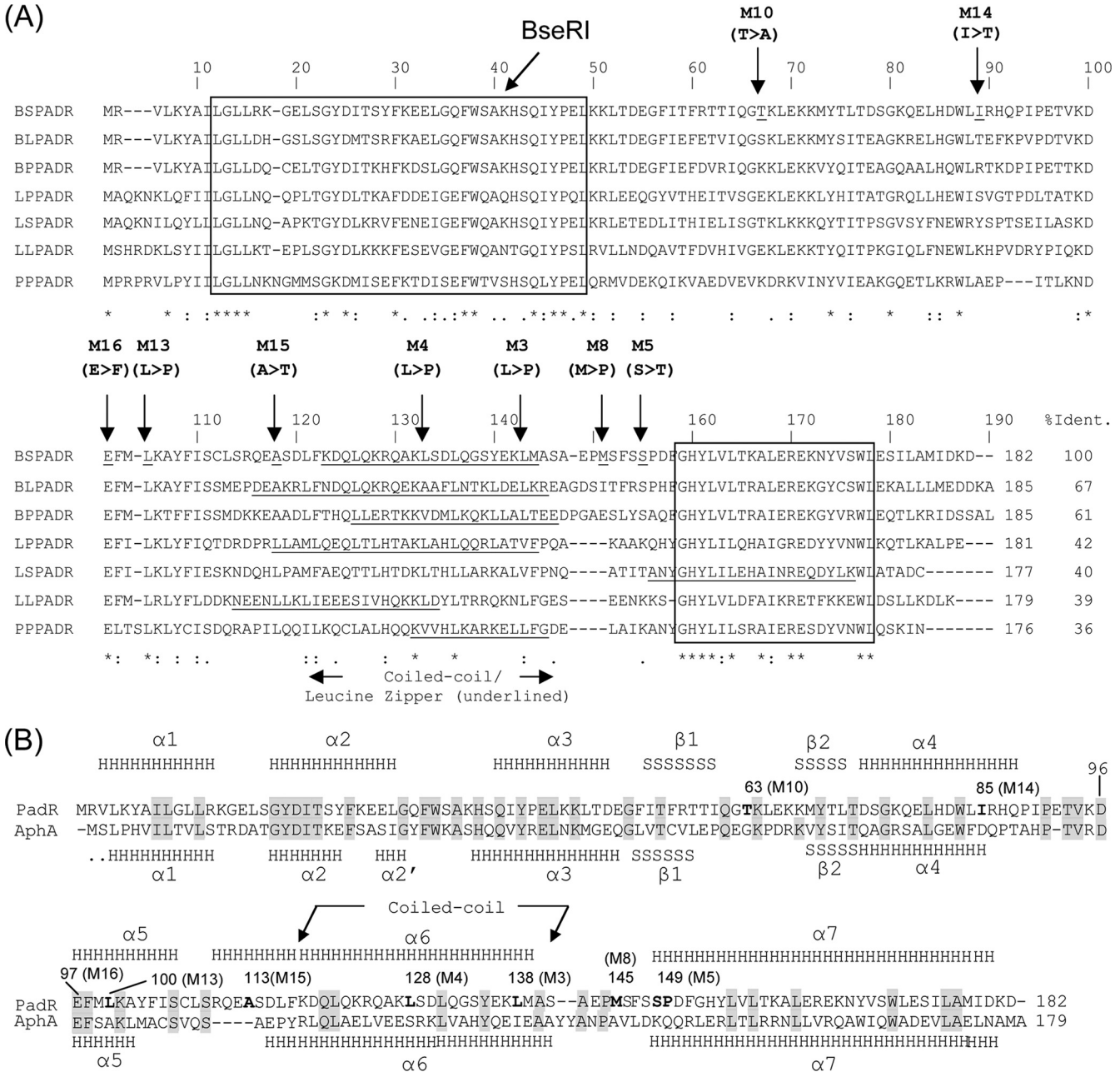

FIG. 7. (A) Multiple alignment of PadRs displaying the highest identity (% Ident.) to PadR from *B. subtilis* 168. BS, *Bacillus subtilis* 168; BL, *Bacillus licheniformis*; BP, *Bacillus pumilus*; LP, *Lactobacillus plantarum*; LS, *Lactobacillus sakei*; LL, *Lactococcus lactis*; PP, *Pediococcus pentosaceus.* Underlined sequences correspond to the putative coiled-coil leucine zipper motif predicted with COILS software (23). Conserved N- and C-terminal sequences are boxed. Vertical arrows indicate the positions of modified amino acid residues. The mutation in M16, which is a representative of the group 3 PadRs that are incapable of repressing *padC* expression, is at the site 97 (E) conserved residue. *, conserved residue. (B) Alignment and prediction of secondary structures (PSIPRED software) for *B. subtilis* 168 PadR and AphA from *Vibrio cholerae* (18). Gray boxed letters are conserved residues.

the binding of two PadR dimers, one with the first dyad, dIR1-2bis, and a second with the second dyad, IR1-2, as well as additional binding in the region covering the −35 box, is responsible for the complete repression of the *padA* (or *padC*) promoter. In *P. pentosaceus*, basal expression of *padR* is likely necessary under NI conditions to produce PadR and to autoregulate the promoter.

To study whether PadR could be involved in regulating other genes, the consensus IR1-2 sequence was screened in the *B. subtilis* 168 strain by using PredictRegulon software (34). Bioinformatic analysis revealed an IR1-2 (ATGTaaatagttACAT) sequence present in the promoter regions of several genes from *B. subtilis* 168, among which the best score was obtained for a sequence in the promoters of the *rbsRKDACB* ribose operon (ATGTaaatagctACAT) (33), the *bioA* gene, and two genes (*yesO* and *ydaI*) of unknown function (http://genolist.pasteur.fr

/SubtiList/) (data not shown). In these promoters, the 8-nt spacer between IR1 and IR2 is fairly conserved. For example, only one substitution is observed in the *rbsRKDACB* promoter. An intriguing future area of study will be the possible interplay between PadR and the expression of the *rbsRKDACB* operon, since this operon is involved in the metabolism of ribose, an essential component of RNA and key compounds of other metabolic pathways.

By random mutagenesis of the *padR* gene, we generated nine different *padR* mutants of interest and identified crucial sites for PadR function. These sites included residue 104 (L) in M13 from group 2 and residue 97 (E) in M16 from group 3. Both of these residues correspond to highly conserved residues in the PadR protein family (Fig. 7). Our findings suggest that these residues are essential for PadR function. In addition, residue 97 (E), which is also present in the α5 helix of AphA, has an identical location in PadR (Fig. 7B). Surprisingly, substitutions in the last 39 residues, including the most conserved C-terminal box, did not result in an interesting phenotype for our study. Similar findings have been shown for random mutagenesis of AphA from *V. cholerae* (18). We therefore hypothesize that either this C-terminal conserved region of PadR-like proteins is assimilated into a family signature not involved in the specific function of the PadR-like subfamily proteins or, conversely, mutations in this region cause severe conformational defects, resulting in product instability. Due to the strategy used for cloning *padR* mutant genes into the native BseRI site, we did not generate a mutant for the first 110 nucleotides of *padR*. As shown for AphA (11), this section might contain residues responsible for binding to the *padC* promoter. Future studies will require directed single codon substitutions in the conserved N-terminal domain without altering PadR structure to determine if this section is involved in binding to the *padC* promoter and then to determine which residues are essential for binding.

Although the overall primary amino acid sequence identity between PadR and AphA is low (28%) compared to that for other PadRs involved in the PASR, the predicted structure of PadR from *B. subtilis* 168 shares a high degree of resemblance with that of AphA, although at present there is no PASR described for *V. cholerae*. The DNA-binding domain of AphA, a region from residue 1 to residue 86, forms a WHTH DNA-binding domain of the GntR superfamily of transcriptional regulators, containing over 6,000 members distributed among almost all bacterial species, both eukaryotes and archaea. The GntR-like proteins bind to promoters as dimers, where each monomer recognizes a half-site of 2-fold symmetric DNA sequence. This is in accordance with our finding by EMSA of different sizes of complexes formed with increasing concentrations of PadR. PadR contains the structural elements α1, α2, α3, α4, β1, and β2. The amino acids which have been identified as important for DNA-binding activity of AphA, for example, G18, Y19, G30, H37, Q39, Y41, K63, and K37 (18), are conserved in PadR. The dimerization domain, including amino acids 98 to 179, forms a coiled-coil motif and corresponds to the structural elements α5, α6, and α7. This AphA motif of the dimerization domain is not similar to that of any other members of the PadR protein family (11).

In conclusion, the IR1-8N-IR2 DNA sequence, which corresponds to one of the two dyads formed by the dIR1-2bis/IR1-2 sequence, is present in all *padC* (or *padA*) promoters to which PadR binds. It is found in the promoter regions of several other genes in *B. subtilis* 168 and other bacteria, in particular *Lactococcus lactis*, *Bacillus anthracis*, and *V. cholerae* (*aphA* gene). Our findings suggest that PadR might modulate the expression of these genes, whose expression might be required directly or indirectly to reduce injury during the PASR. To decipher if PadR is a pleiotropic regulator, further interests of our group include (i) screening the entire genomes of *B. subtilis* 168 and other species, with or without PASR activity, for native or degenerate versions of dIR1-2bis/IR1-2; (ii) testing the interaction of PadR with modified *padC* promoters containing single nucleotide modifications in the dIR1-2bis/IR1-2 sequence but also in the whole protected sequence with 10 nM PadR to determine mutations that cause binding participating in repression under NI conditions; and (iii) proteomic studies with wild-type and mutant *padR* variants of *B. subtilis* 168 to compare phenolic acid-induced and noninduced proteomes.

ACKNOWLEDGMENTS

T. K. C. Nguyen and N. P. Tran were supported by Ph.D. grants from the French Embassy in Vietnam. This work was also partially supported by the Conseil Régional de Bourgogne.

We are grateful to Marta Perego (The Scripps Research Institute, La Jolla, CA) and Didier Lereclus (Institut Pasteur and INRA, France) for generously providing vectors. We thank Christine Rojas for her technical assistance.

REFERENCES

1. **Agustiandari, H., J. Lubelski, H. B. van den Berg van Saparoea, O. P. Kuipers, and A. J. M. Driessen.** 2008. LmrR is a transcriptional repressor of expression of the multidrug ABC transporter LmrCD in *Lactococcus lactis*. J. Bacteriol. **190:**759–763.
2. **Alekshun, M. N., S. B. Levy, T. R. Mealy, B. A. Seaton, and J. F. Head.** 2001. The crystal structure of MarR, a regulator of multiple antibiotic resistance, at 2.3 A resolution. Nat. Struct. Biol. **8:**710–714.
3. **Arantes, O., and D. Lereclus.** 1991. Construction of cloning vectors for *Bacillus thuringiensis*. Gene **108:**115–119.
4. **Aravind, L., V. Anantharaman, S. Balaji, M. M. Babu, and L. M. Iyer.** 2005. The many faces of the helix-turn-helix domain: transcription regulation and beyond. FEMS Microbiol. Rev. **29:**231–262.
5. **Arita, K., et al.** 2007. Structural and biochemical characterization of a *Cyanobacterium circadian* clock-modifier protein. J. Biol. Chem. **282:**1128–1135.
6. **Barthelmebs, L., C. Diviès, and J.-F. Cavin.** 2000. Knockout of the *p*-coumarate decarboxylase gene from *Lactobacillus plantarum* reveals the existence of two other inducible enzymatic activities involved in phenolic acid metabolism. Appl. Environ. Microbiol. **66:**3368–3375.
7. **Barthelmebs, L., B. Lecomte, C. Diviès, and J.-F. Cavin.** 2000. Inducible metabolism of phenolic acids in *Pediococcus pentosaceus* is encoded by an autoregulated operon which involves a new class of negative transcriptional regulator. J. Bacteriol. **182:**6724–6731.
8. **Cavin, J.-F., L. Barthelmebs, and C. Diviès.** 1997. Molecular characterization of an inducible *p*-coumaric acid decarboxylase from *Lactobacillus plantarum*: gene cloning, transcriptional analysis, overexpression in *Escherichia coli*, purification, and characterization. Appl. Environ. Microbiol. **63:**1939–1944.
9. **Cavin, J.-F., V. Dartois, and C. Diviès.** 1998. Gene cloning, transcriptional analysis, purification, and characterization of phenolic acid decarboxylase from *Bacillus subtilis*. Appl. Environ. Microbiol. **64:**1466–1471.
10. **Christov, L. P., and B. A. Prior.** 1993. Esterases of xylan-degrading microorganisms—production, properties, and significance. Enzyme Microb. Technol. **15:**460–475.
11. **De Silva, R. S., et al.** 2005. Crystal structure of the virulence gene activator AphA from *Vibrio cholerae* reveals it is a novel member of the winged helix transcription factor superfamily. J. Biol. Chem. **280:**13779–13783.
12. **de Vries, R. P., C. B. Faulds, and J. Visser.** 1999. The *faeA* gene from *Aspergillus niger* encoding a feruloyl esterase with activity on xylan and pectin is subject to a complex system of regulation. J. Sci. Food Agric. **79:**443–446.
13. **Dower, W. J., J. F. Miller, and C. W. Ragsdale.** 1988. High efficiency transformation of *Escherichia coli* by high voltage electroporation. Nucleic Acids Res. **16:**6127–6145.

14. **Gury, J., L. Barthelmebs, N. P. Tran, C. Diviès, and J.-F. Cavin.** 2004. Cloning, deletion, and characterization of PadR, the transcriptional repressor of the phenolic acid decarboxylase-encoding *padA* gene of *Lactobacillus plantarum*. Appl. Environ. Microbiol. **70:**2146–2153.
15. **Gury, J., et al.** 2009. Inactivation of PadR, the repressor of the phenolic acid stress response, by molecular interaction with Usp1, a universal stress protein from *Lactobacillus plantarum*, in *Escherichia coli*. Appl. Environ. Microbiol. **75:**5273–5283.
16. **Hirooka, K., et al.** 2007. Dual regulation of the *Bacillus subtilis* regulon comprising the lmrAB and yxaGH operons and yxaF gene by two transcriptional repressors, LmrA and YxaF, in response to flavonoids. J. Bacteriol. **189:**5170–5182.
17. **Huillet, E., P. Velge, T. Vallaeys, and P. Pardon.** 2006. LadR, a new PadR-related transcriptional regulator from *Listeria monocytogenes*, negatively regulates the expression of the multidrug efflux pump MdrL. FEMS Microbiol. Lett. **254:**87–94.
18. **Kovacikova, G., W. Lin, and K. Skorupski.** 2004. *Vibrio cholerae* AphA uses a novel mechanism for virulence gene activation that involves interaction with the LysR-type regulator AphB at the *tcpPH* promoter. Mol. Microbiol. **53:**129–142.
19. **Kovacikova, G., W. Lin, and K. Skorupski.** 2003. The virulence activator AphA links quorum sensing to pathogenesis and physiology in *Vibrio cholerae* by repressing the expression of a penicillin amidase gene on the small chromosome. J. Bacteriol. **185:**4825–4836.
20. **Kovacikova, G., and K. Skorupski.** 2001. Overlapping binding sites for the virulence gene regulators AphA, AphB and cAMP-CRP at the *Vibrio cholerae tcpPH* promoter. Mol. Microbiol. **41:**393–407.
21. **Lavrrar, J. L., and M. A. McIntosh.** 2003. Architecture of a Fur binding site: a comparative analysis. J. Bacteriol. **185:**2194–2202.
22. **Lin, K.-C., and D. Shiuan.** 1995. A simple method for DNaseI footprinting analysis. J. Biochem. Biophys. Methods **30:**85–89.
23. **Lin, W., G. Kovacikova, and K. Skorupski.** 2007. The quorum sensing regulator HapR downregulates the expression of the virulence gene transcription factor AphA in *Vibrio cholerae* by antagonizing Lrp- and VpsR-mediated activation. Mol. Microbiol. **64:**953–967.
24. **Lupas, A., M. Vandyke, and J. Stock.** 1991. Predicting coiled coils from protein sequences. Science **252:**1162–1164.
25. **Madoori, P. K., H. Agustiandari, A. J. M. Driessen, and A. Thunnissen.** 2009. Structure of the transcriptional regulator LmrR and its mechanism of multidrug recognition. EMBO J. **28:**156–166.
26. **McGuffin, L. J., K. Bryson, and D. T. Jones.** 2000. The PSIPRED protein structure prediction server. Bioinformatics **16:**404–405.
27. **McSweeney, C. S., A. Dulieu, R. I. Webb, T. Del Dot, and L. L. Blackall.** 1999. Isolation and characterization of a *Clostridium sp*. with cinnamoyl esterase activity and unusual cell envelope ultrastructure. Arch. Microbiol. **172:**139–149.
28. **Msadek, T., et al.** 1998. ClpP of *Bacillus subtilis* is required for competence development, motility, degradative enzyme synthesis, growth at high temperature and sporulation. Mol. Microbiol. **27:**899–914.
29. **Nguyen, V. D., et al.** 2007. The proteome and transcriptome analysis of *Bacillus subtilis* in response to salicylic acid. Proteomics **7:**698–710.
30. **Perego, M.** 1993. Integrational vectors for genetic manipulations in *Bacillus subtilis*, p. 615–624. *In* A. L. Sonensheim, J. A. Hoch, and R. Losick (ed.), *Bacillus subtilis* and other Gram-positive bacteria: biochemistry, physiology, and molecular genetics. American Society for Microbiology, Washington, DC.
31. **Sambrook, J., E. F. Fritsch, and T. Maniatis.** 1989. Molecular cloning: a laboratory manual, 2nd ed., vol. 1. Cold Spring Harbor Laboratory, Cold Spring Harbor, NY.
32. **Tran, N. P., et al.** 2008. Phenolic acid-mediated regulation of the *padC* gene, encoding the phenolic acid decarboxylase of *Bacillus subtilis*. J. Bacteriol. **190:**3213–3224.
33. **Woodson, K., and K. M. Devine.** 1994. Analysis of a ribose transport operon from *Bacillus subtilis*. Microbiology **140:**1829–1838.
34. **Yellaboina, S., J. Seshadri, M. S. Kumar, and A. Ranjan.** 2004. PredictRegulon: a web server for the prediction of the regulatory protein binding sites and operons in prokaryote genomes. Nucleic Acids Res. **32:**W318–W320.
35. **Zhang, C. M., J. Nietfeldt, M. Zhang, and A. K. Benson.** 2005. Functional consequences of genome evolution in *Listeria monocytogenes*: the *lmo0423* and *lmo0422* genes encode sigma(C) and LstR, a lineage II-specific heat shock system. J. Bacteriol. **187:**7243–7253.